ISBN: 978-3-95450-231-8 ISSN: 2673-5490 doi: https://doi.org/10.18429/JACoW-IPAC-23-THPL150

DEALING WITH THERMIONIC EMISSION IN WIRE SCANNERS BASED ON SECONDARY ELECTRON EMISSION

M. Boucard, École polytechnique fédérale de Lausanne, Lausanne, Switzerland
M. Sapinski*, Paul Scherrer Institut, Villigen, Switzerland

Abstract

Measurement of transverse beam profiles using thin wires is a very successful and widely used method. The signal is generated by measuring scattered particles outside the vacuum chamber or by measuring the current of the secondary electrons emitted from the wire. In high-brightness accelerators, the heating of the wire induced by direct beam interaction or by coupling to RF fields can lead to the thermionic emission of electrons, which disturbs the secondary electron current measurement. The spectra of the electrons are different, but they overlap, therefore the typically used method of biasing the wire only partly reinstates the original beam profile. This study investigates the mixing of current from both phenomena and attempts to address the question of the optimal bias voltage. The estimations are compared to measurements performed on high-brightness beams of PSI Main Ring cyclotron.

INTRODUCTION

Wire scanners are devices in which a thin wire moves through a beam probing its transverse profile. When the beam particles interact with the wire material, they generate secondary particles that are measured. Correlating the measurement of the flux of secondary particles with the wire position allows for reconstruction of beam profile.

Secondary particles in high-energy machines can be measured by scintillators outside of the vacuum chamber. However, low-energy beams do not generate enough high-energy secondaries, and the current of secondary electrons (SE) is measured instead.

Most of the energy deposited by the beam in the material takes the form of heat. Hot wires emit thermal electrons, and the intensity of the emitted current is not proportional to the density of beam particles. Therefore, the presence of thermionic emission disturbs the measurement.

The PSI's Main Ring Long Radial Probe (RRL) is a type of wire scanner which is able to scan all the orbits along the cyclotron radius [1]. The beam in Main Ring Cyclotron is made of protons and makes more than 180 revolutions over a radius of 2.5 m from injection at 72 MeV to extraction at 590 MeV. The beam intensity can reach 2.2 mA. Carbon fibers, with 34 µm diameter, are used as probes. They operate at high temperatures, and thermionic emission is often evident. It is suppressed using a positive bias of the wire. The setup of the bias voltage value, understanding how it works, and the role of beam potential are discussed here.

* mariusz.sapinski@psi.ch

SECONDARY AND THERMIONIC EMISSION

The intensity of SE is well described by the Sternglass model [2]. The original paper only qualitatively discusses the expected properties of the electron spectrum, mentioning that it should not strongly depend on the material type (work function and density of conduction electrons). The literature contains numerous measurements of the spectra as well as theoretical formulas [3,4]. Typically, the SE spectrum peaks at 1-2 eV and has a long high-energy tail. The emission of secondary electron takes place in the first few nanometers of the target surface and is usually a prompt process, with electrons leaving the target within femtoseconds.

The intensity of thermionic current is described by the Richardson-Dushman formula and is very strongly dependent on the temperature. The distribution of the kinetic energy of thermionic electrons follows the high-energy tail of the Fermi-Dirac distribution of electrons in solid material. At temperatures typical for RRL wires, the kinetic energies of emitted thermionic electrons are lower than those of secondary electrons. The thermionic emission extends over the time the target remains hot. In the case of RRL it is about 0.1 s per measured orbit.

EXPERIMENTAL CONDITIONS

The conditions inside the PSI Main Ring are the following:

- vacuum of about 10^{-6} mbar;
- strong fields leaking from the RF cavities and coupling to wires; the wires are glowing even without the beam and it is estimated that they are preheated to about 1000 K (see Fig. 6 in [5]);
- strong radiation;
- bunch length is between 20 mm (1 sigma of the core) and 200 mm (total length) [6];
- bunch spacing 20 ns;
- beam intensity between 5 and 1800 µA [1] what corresponds to bunch population between $6.25 \cdot 10^5$ and $2.25 \cdot 10^8$ protons per bunch;
- transverse bunch size of the order of 1 mm.

The wires are biased using batteries, which do not generate electronic noise. The various configurations of the

[1] Maximum beam current was limited in 2022 due to problems with one of the Injector resonators.

ISBN: 978-3-95450-231-8 ISSN: 2673-5490 doi: https://doi.org/10.18429/JACoW-IPAC-23-THPL150

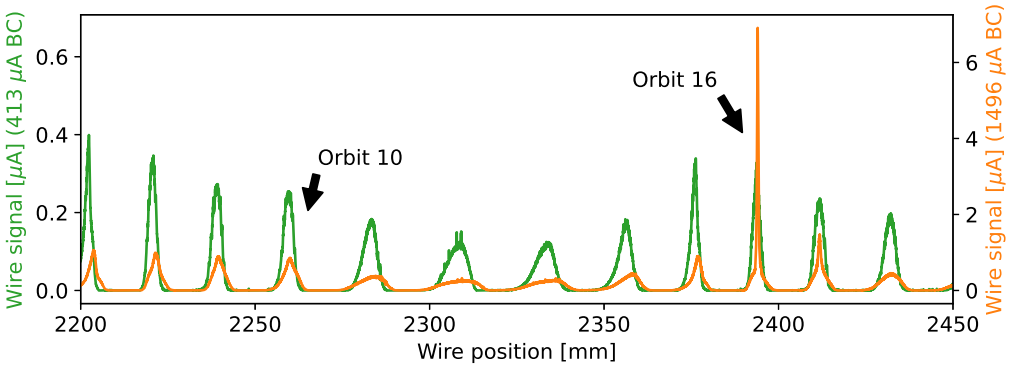

Figure 1: A fragment of RRL signal measured with wire 1 with the two analysed peaks marked. Lack of the bias voltage lead to excessive signal for high-intensity scan (orange line). Scan direction from right to left (inward scan).

batteries allow to generate bias voltages of 30, 60, 90 V, but tests were also done with 120 V and even 300 V. However, not all data points are available for all wires. The current readout is performed using MESON logarithmic amplifier modules [7]. Its response function introduces a slight asymmetry in the signal.

The subsequent analysis is focused on low-energy orbits (10 and 16), because they are clearly separated, while at high energies the profiles overlap. Only data from the inwards movement are used as they have lower noise. A small fragment of the total profile, which extends from 2046.2 mm to 4574.1 mm is shown in Fig. 1.

The RRL is equipped with 3 carbon fiber wires: one vertical and two tilted by $\pm 45°$. The horizontal beam profile (σ_H) is measured directly by vertical wire, while the width of the vertical beam profile (σ_V) is derived from tilted wires 2 and 3 (σ_D) using Equation:

$$\sigma_V = \sqrt{\frac{\sigma_H^2 \sigma_D^2}{2\sigma_H^2 - \sigma_D^2}} \tag{1}$$

The above relation assumes that the transverse profiles are Gaussian. Observation of the measured profiles often shows distortions from the Gaussian shape, and this is not taken into account in the simulations. In addition, the presence of thermionic emission at high intensities makes it difficult to estimate beam sigma. In those cases, σ_H and σ_V are derived from measurements at low intensity using a dependence established from numerous measurements made on various detectors along the beam [8]:

$$\sigma_{H,V}(I_{beam}) = a I_{beam}^{\frac{1}{3}} \tag{2}$$

with a, a constant determined with low current profiles.

The parameters of the profiles analyzed are summarized in Table 1. Profile number 10 is broader and shows no or weak thermionic emission, while profile 16 was chosen because of a strong thermionic component.

SIMULATIONS

A debugged and improved version of the pyTT package [9] is used to simulate the secondary electron emission yield, the temperature of the wire and the thermionic current [10]. Simulations take into account the temperature dependence of specific heat, emissivity, and work function. An example of simulation results overlapped with the measured data is shown in Fig. 2. The scan direction is from left to right. The simulation systematically gives slightly higher results than the measurements, what can be an instrumental effect. Bunch potential for various orbits is computed using a simple PIC algorithm assuming single bunch in an empty space. In reality the potentials of bunches on other orbits add up leading to higher values and playing a crucial role in electron transport out of the wire.

DISCUSSION

Thermionic Emission

Figure 3 shows a comparisons of beam profiles measured and simulated for orbit number 10 (105 MeV) and 16 (123 MeV), for beam current of 1496 µA and without bias voltage. The profile of orbit number 10 features a small additional thermionic current which is correctly modeled by the simulations. However, in case of orbit number 16 the thermionic emission peak is much higher, and the simulation does not reproduce it correctly. Two simulated curves show the results obtained with different parameterizations of the dependence of the work function on temperature. Using the

Table 1: Parameters of the Measured Profiles Used in the Simulations

Peak (or orbit) Nr	**10**		**16**	
Beam energy [MeV]	105.6		123	
dE/dx [MeV cm^2 g^{-1}]	6.231		5.575	
Beam current [µA]	413	1496	413	1496
σ_H [mm]	1.348	2.071	1.064	1.633
σ_V [mm]	1.031	1.583	0.9127	1.402

ISBN: 978-3-95450-231-8 ISSN: 2673-5490 doi: https://doi.org/10.18429/JACoW-IPAC-23-THPL150

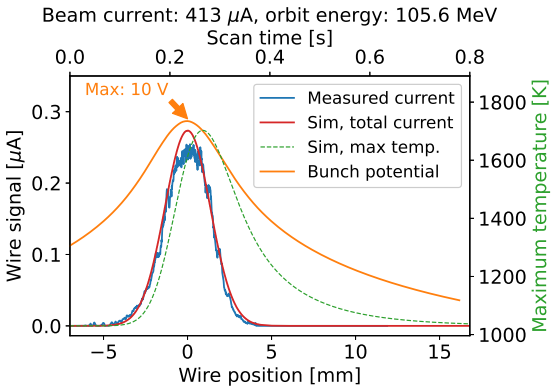

Figure 2: Wire signal for 413 µA beam current for orbit number 10. Temperature in the wire center reaches 1700 K, no thermionic emission is observed.

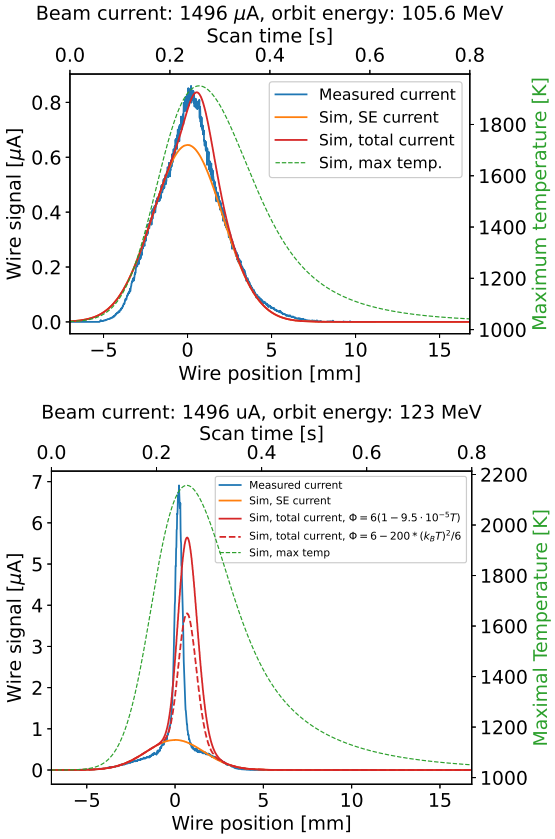

Figure 3: Measurements and simulations of the wire signal for 1496 µA beam current for orbits number 10 and 16.

quadratic dependence: $\Phi(T) = \Phi(T_0) - \gamma \frac{k_B T^2}{\Phi(T_0)}$, as suggested in [11], leads to a better agreement. The remaining discrepancy is probably due to a buildup of space charge and increase of electron reflection coefficient, which reflects the forces driving electrons back to the wire.

Bias Voltage

Biasing the wire with a positive potential is expected to cut the thermionic emission, however it should also affect

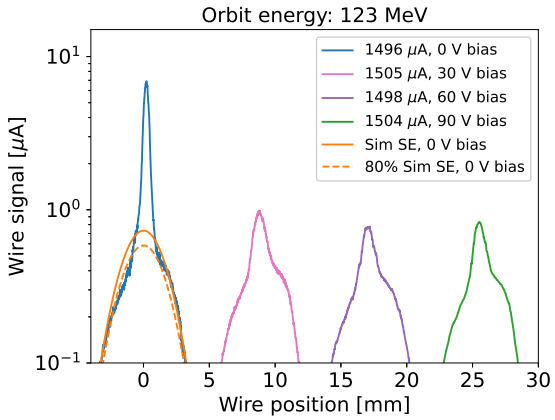

Figure 4: Wire signal for different bias voltage for orbit number 16 at high beam current.

SE. Figure 4 shows the expected and measured wire currents. Already 30 V bias partly suppresses the thermionic emission however, the remaining "bump" is not affected by further increase of the bias. The bias reduces the thermionic current to about 8% of the initial value. It also affects the SE current, but to a much smaller degree.

CONCLUSIONS

At first, the mechanism of applying a bias voltage to a wire scanner seems to simply relay the idea of bringing back low-energy thermionic electrons to the wire. This is true when the bunches do not overlap with the wire. However, when a bunch passes the wire, both thermionic and secondary electrons contribute to the signal. As SE are generated promptly, most of them are affected by the bunch potential that leads to their liberation from the wire. This is why the SE signal is very weakly affected by the value of wire bias. The thermionic electrons are emitted continuously also between the bunches, however due to the same mechanism as SE, they can only escape when the bunch is present, that is, for about 8% of time. Therefore, the application of wire bias reduces the thermionic signal by more than 90%, but the remaining signal cannot be removed by increasing the bias within a reasonable range.

The exact mechanism which leads to the liberation of low-energy electrons from a biased wire require detailed tracking simulations of electrons exposed to transient field of the bunch together with field of the wire. This will also help to understand the deformation of the measured profiles caused by the angle between bunch field and the wire direction. Further measurements with additional levels of the wire bias are also planned.

ACKNOWLEDGEMENTS

Authors would like to thank R. Doelling for inspiring the study and for numerous fruitful discussions.

ISBN: 978-3-95450-231-8 ISSN: 2673-5490 doi: https://doi.org/10.18429/JACoW-IPAC-23-THPL150

REFERENCES

[1] M. Sapinski, R. Dölling, and M. Rohrer, "Commissioning of the Renewed Long Radial Probe in PSI Ring Cyclotron", in *Proc. IBIC'22*, Kraków, Poland, Sep. 2022, pp. 76–79. doi:10.18429/JACoW-IBIC2022-MOP19

[2] E. J. Sternglass, "Theory of Secondary Electron Emission by High-Speed Ions", *Phys. Rev.*, vol. 108, pp. 1–12, 1957. doi:10.1103/PhysRev.108.1

[3] D. Hasselkamp, S. Hippler and A. Scharmann, "Ion-induced secondary electron spectra from clean metal surfaces", *Nucl. Instrum. Methods Phys. Res., Sect. B*, vol. 18, pp. 561–565, 1986. doi:10.1016/S0168-583X(86)80088-X\textbf

[4] M. S. Chung, T. E. Everhart, "Simple calculation of energy distribution of low-energy secondary electrons emitted from metals under electron bombardment", *J. Appl. Phys.*, vol. 45, pp. 707–709, 1974. doi:10.1063/1.1663306

[5] M. Sapinski, R. Dölling, and M. Rohrer, "Commissioning of the Renewed Long Radial Probe in PSI Ring Cyclotron", in *Proc. IBIC'22*, Kraków, Poland, Sep. 2022, pp. 76–79. doi:10.18429/JACoW-IBIC2022-MOP19

[6] R. Dölling, "Bunch-Shape Measurements at PSI's High-power Cyclotrons and Proton Beam Lines", in *Proc. Cyclotrons'13*, Vancouver, Canada, Sep. 2013, paper TU3PB01, pp. 257–261.

[7] E. Johansen, "VME Meson design specification", PSI, Villigen, Switzerland, June 2010, unpublished

[8] Ch. Baumgarten and H. Zhang, private communication, 2023.

[9] A. Navarro, "Understanding Secondary Emission Processes and Beam Matter interactions for Optimization of Diagnostic Wire Grid System in Particle Accelerators", Ph.D. thesis, Universitat Politecnica de Catalunya, Barcelona, Spain, 2023.

[10] M. Sapinski, "Model of carbon wire heating in accelerator beam", CERN, Geneva, Switzerland, Rep. CERN AB-2008-030-BI, 2008.

[11] R. Rahemi and D. Li, "Variation in electron work function with temperature and its effect on the Young's modulus of metals", *Scr. Mater.*, vol. 99, pp. 41–44, 2015.